Turkish Journal of Engineering

https://dergipark.org.tr/en/pub/tuje

e-ISSN 2587-1366

Improved hybrid intelligent controller design for MPPT of stand-alone PV System

O. Fatih Kececioglu[1], Ahmet Gani *[1], Mustafa Sekkeli [1]

[1]*Kahramanmaras Sutcu Imam University, Engineering and Architecture Faculty, Department of Electrical and Electronics Engineering, Kahramanmaraş, Turkey*

Keywords
Hybrid intelligent controller
MPPT
Stand-alone PV system

ABSTRACT

Photovoltaic (PV) systems have low power conversion efficiency, so maximum power point tracking (MPPT) control methods are utilized to maximize the efficiency of PV systems. The present study proposes an improved hybrid intelligent controller design for the MPPT of stand-alone PV system. The hybrid intelligent control structure is integrated into Angle of Incremental Conductance (AIC) method and Interval Type-2 Takagi-Sugeno-Kang Fuzzy Logic Controller (IT2-TSKFLC). The proposed hybrid intelligent controller offers a superior performance in terms of dealing with uncertainties of sudden changes under different environmental conditions. A simulation model is created in Matlab/Simulink using daily data from a real solar PV plant to evaluate the performance of the proposed hybrid intelligent controller. The simulation findings demonstrated that the proposed hybrid intelligent controller displays a highly stable and robust performance in terms of tracking maximum power point compared to a conventional AIC MPPT method against various uncertainties stemming from disturbing inputs such as solar irradiance and panel temperature variations.

1. INTRODUCTION

Solar energy is a clean, abundant and sustainable energy source which bears a great potential for energy needs in the future. Photovoltaic (PV) power generation has become very widespread around the world (Dogmus et al. 2017). However, PV power generation systems have three main drawbacks: high installation cost, low power conversion efficiency and high dependence on environmental conditions such as solar irradiance and temperature.

In general, a PV panel, power converter, and load can be found in a basic PV system. Power converter is the most crucial component of a PV system. In the existing literature, various power converter topologies are used for PV systems. A power converter controls the power flow from a PV panel to the load (Kececioglu et al. 2018). Buck, Boost and Buck-Boost converter, which is also known as conventional power DC-DC converters, are among the most widely used power converter topologies. Conventional DC-DC power converters offer a limited output voltage and power transfer efficiency because of parasitic elements in their circuit topology. Therefore, high voltage conversion gain DC-DC power converters eliminate this problem. Voltage lift technique overcomes parasitic elements for high voltage conversion gain DC-DC power converters. Luo converters provide several advantages such as a higher output voltage, power density, efficiency and a lower output voltage ripple (Luo 1997). In the present study, Modified Positive Output Luo Converter (MPOLC) with re-lift configuration is used to provide high voltage gain conversion.

Current-Voltage (I-V) and Power-Voltage (P-V) characteristic curves of a PV panel are non-linear and vary depending on environmental conditions. On these curves is an optimum power point called maximum power point (MPP) and thus the PV panel generates maximum output power at the MPP (Dixit et al. 2018). MPPT control methods enable PV systems to overcome high dependence on environmental conditions. In the existing literature, MPPT methods are divided into two categories as conventional and intelligent methods. While Hill-climbing (HC), perturb and observe (P&O), incremental conductance (IC) and angle of incremental conductance (AIC) are conventional MPPT methods, Artificial Neural Network (ANN) and Fuzzy Logic (FL) are

* **Corresponding Author**

(fkececioglu@ksu.edu.tr) ORCID ID 0000 – 0001 – 7004 – 4947
*(agani@ksu.edu.tr) ORCID ID 0000 – 0002 – 6487 – 6066
(msekkeli@ksu.edu.tr) ORCID ID 0000 – 0002 – 1641 – 3243

Cite this article

Kececioglu O F, Gani A & Sekkeli M (2021). Improved HYBRID intelligent controller design for MPPT of stand-alone PV System. Turkish Journal of Engineering, 5(1), 20-28

Research Article / DOI: 10.31127/tuje.652229

Received: 28/11/2019; Accepted: 18/01/2020

intelligent MPPT methods (Soon and Mekhilef 2015). Conventional MPPT methods pose some problems such as continuous oscillation, low tracking speed and power losses around MPP. Intelligent MPPT methods, however, offer a high tracking speed, accuracy and efficiency (Radjai et al. 2015).

Type-2 Fuzzy Logic System (T2FLS) has been recently used to overcome uncertainties in the modeling process. The output power of a PV panel depends on solar irradiance and panel temperature affected by atmospheric conditions, leading to uncertainties in the operation of a PV system. Compared to Type-1 Fuzzy Logic System (T1FLS) in a PV system, T2FLS is more successful when it comes to handling uncertainties (Kumbasar 2016).

In the present study, a new improved hybrid intelligent controller is proposed in order to reach maximum power of a PV panel with minimum oscillations and the highest tracking speed under all environmental conditions. The proposed hybrid intelligent controller for the MPPT of the PV system relies on the AIC and Interval Type-2 Takagi-Sugeno-Kang Fuzzy Logic Controller (AIC IT2-TSKFLC).

The present study is organized as follows: MPOLC re-lift configuration for PV system is analyzed in Section 2.The proposed hybrid intelligent controller is presented in Section 3. Simulation studies and dynamic performance of the proposed method are discussed in Section 4. Finally, the conclusions of the study are explained in Section 5.

2. ANALYSIS OF MPOLC RE-LIFT CONFIGURATION FOR PV SYSTEM

The output voltage of a single PV panel does not suffice for on-grid or off grid-connected PV systems, and thus it must be increased, which requires a higher voltage level provided by the series connection of PV panels. However, the number of series-connected PV panels may bring about limitations in practice such as PV voltage isolation, efficiency and shadowing effect. As a result, step-up converters such as MPOLC are essential to provide high voltage conversion gain for PV systems (Ozdemir et al. 2017).The proposed MPOLC re-lift configuration performs the MPPT of a PV system without needing any additional DC/DC converter, and prevents losses caused by an additional DC/DC converter. MPOLC in a re-lift configuration is derived from the positive output Luo converter in a self-lift configuration. Instead of using two switches in the positive output Luo converter, MPOLC in re-lift configuration uses a single switch to perform a DC-DC step-up voltage conversion. The voltage lift technique improves circuit properties. MPOLC is analyzed operating in the continuous conduction mode. Circuit elements of MPOLC are assumed to be ideal when steady-state analysis is carried out (Kececioglu 2019). The steady-state analysis is carried for two different modes: switch-on and switch-off. MPOLC with a re-lift configuration is shown in Fig. 1.*Vs* is the input voltage, and V_L is the load voltage of MPOLC.

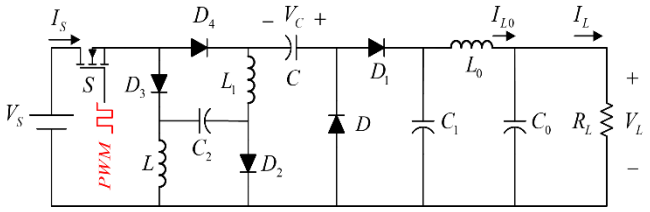

Figure 1. Modified positive output Luo converter with re-lift configuration

2.1. Analysis for Mode-1: Switch-On

The equivalent circuit of MPOLC for the switch-on mode is shown in Fig.2. In the switch-on mode, *D1-D2-D3-D4* diodes are forward biased, while D diode is reverse biased.

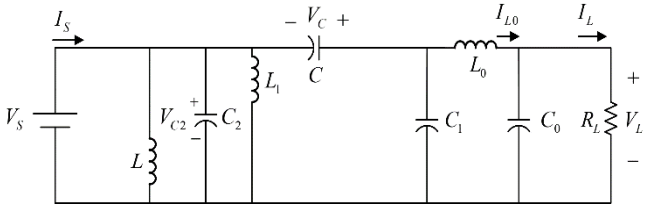

Figure 2. Equivalent circuit for switch-on

The voltage across the inductors *L* and *L1* are equal to input voltage (V_S). The voltage across capacitor C_2, V_{C2} is also equal to V_S, and defined as:

$$v_L = L\frac{di_L}{dt} = v_{L1} = L_1\frac{di_{L1}}{dt} = V_S = V_{C2} \quad (1)$$

Similarly, inductor L_0 current equation is calculated as:

$$v_{L0} = L_0\frac{dI_{L0}}{dt} = V_{C1} - V_L \quad (2)$$

Using Kirchhoff's voltage law, an equation related voltage across capacitor *C* and C_0 is defined as:

$$V_S + V_C = V_{C1} \quad (3)$$

Current (i_{C0}) through capacitor C_0 is expressed as:

$$i_{C0} = C_0\frac{dv_{C0}}{dt} = I_{L0} - I_L \quad (4)$$

Using Kirchhoff's current law, the current equations for *C*, C_1 and C_2 are calculated as:

$$i_C - i_{C1} = C\frac{dv_C}{dt} - C_1\frac{dv_{C1}}{dt} = I_{L0} \quad (5)$$

$$i_C + i_{C2} = C\frac{dv_C}{dt} + C_2\frac{dv_{C2}}{dt} = I_S - i_L - i_{L1} \quad (6)$$

2.2. Analysis for Mode-1: Switch-Off

The equivalent circuit of MPOLC for the switch off mode is shown in Fig. 3. *D* diode is forward biased and *D1-D2-D3-D4* diodes are reverse biased when S switch is turned off.

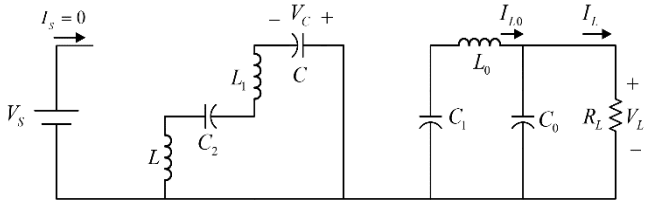

Figure 3. Equivalent circuit for switch-off

The current through the capacitor C_0 is expressed as:

$$i_{C0} = C_0 \frac{dv_{C0}}{dt} = I_{L0} - I_L \tag{7}$$

Similarly, current through capacitors C, C_1 and C_2 are defined as:

$$i_{C1} = C_1 \frac{dv_{C1}}{dt} = -I_{L0} \tag{8}$$

$$i_{C2} = i_C = C_2 \frac{dv_{C2}}{dt} = C\frac{dv_C}{dt} = -i_{L1} = -i_L \tag{9}$$

The voltage across inductors L_0 is calculated as:

$$v_{L0} = L_0 \frac{dI_{L0}}{dt} = V_{C1} - V_L \tag{10}$$

The voltage across inductors L and L_1 are defined as:

$$V_{L-OFF} + V_{L1-OFF} + V_{C2} - V_C = 0 \tag{11}$$

or

$$v_L = L\frac{di_L}{dt} = V_{L1-OFF} + V_{C2} - V_C \tag{12}$$

or

$$v_{L1} = L_1 \frac{di_{L1}}{dt} = V_{L-OFF} + V_{C2} - V_C \tag{13}$$

The inductor current i_L increases in the mode-1 period, and decreases in the mode-2 period. V_S and $-V_{L\text{-}OFF}$ are the corresponding voltages across L. Therefore,

$$DTV_I = (1-D)TV_{L-OFF} \tag{14}$$

Therefore,

$$V_{L-OFF} = \frac{D}{1-D}V_S \tag{15}$$

In a similar way, the inductor current i_{L1} increases in the mode-1 period, and decreases in the mode-2 period. The corresponding voltages across L_1 are V_S and $-V_{L1\text{-}OFF}$. Thus,

$$DTV_I = (1-D)TV_{L1-OFF} \tag{16}$$

and

$$V_{L1-OFF} = \frac{D}{1-D}V_S \tag{17}$$

The Eq. 11 can be modified using Eqs. 1, 15 and 16 as follows:

$$\frac{D}{1-D}V_S + \frac{D}{1-D}V_S + V_S - V_C = 0 \tag{18}$$

$$V_C = \frac{1+D}{1-D}V_S \tag{19}$$

Using Eqs. 2-3, the output voltage of converter (V_L) is calculated as:

$$V_L = V_S + V_C \tag{20}$$

$$V_L = V_S + \frac{1+D}{1-D}V_S = \frac{2}{1-D}V_S \tag{21}$$

The voltage transfer ratio (M) is calculated as:

$$M = \frac{V_L}{V_S} = \frac{2}{1-D} \tag{22}$$

2.3. Design Constraints of MPOLC

In MPOLC analysis, element boundary values are calculated using Eqs. 23-30 based on current changes in inductors and voltage changes in capacitors. The variation ratio of the current through inductor L is expressed as:

$$\zeta = \frac{\Delta I_L / 2}{I_L} = \frac{R_L D}{M^2 fL} \tag{23}$$

Similarly, the variation ratio for inductor L_1 is defined as:

$$\zeta_1 = \frac{\Delta I_{L1} / 2}{I_{L1}} = \frac{R_L D}{M^2 fL_1} \tag{24}$$

The variation of the current through diode I_D is given as:

$$\xi = \frac{\Delta I_D / 2}{I_D} = \frac{R_L D}{fL_{eq} M^2} \tag{25}$$

Here, L_{eq} is the equivalent inductance $L//L_1$. The variation ratio of the voltage across the capacitor C is calculated as:

$$\sigma = \frac{\Delta V_C / 2}{V_C} = \frac{1}{fCR_L(1+D)} \tag{26}$$

In a similar way, the variation ratio for capacitor C_1 is defined as:

$$\sigma_1 = \frac{\Delta V_{C1} / 2}{V_{C1}} = \frac{1}{fC_1 R_L M} \tag{27}$$

The variation ratio for the capacitor C_2 is expressed as:

$$\sigma_2 = \frac{\Delta V_{C2}/2}{V_{C2}} = \frac{M}{2fC_2R_L} \quad (28)$$

The variation ratio of the current through the inductor L_0 is calculated as:

$$\zeta_0 = \frac{\Delta I_{L0}/2}{I_{L0}} = \frac{1}{8f^2C_1ML_0} \quad (29)$$

Finally, the variation ratio of the voltage across the capacitor C_0 is expressed as:

$$\sigma_0 = \frac{\Delta V_{CO}/2}{V_{CO}} = \frac{1}{64R_LMf^3L_0C_0C_1} \quad (30)$$

The boundary between continuous conduction mode (CCM) and discontinuous conduction mode (DCM) is calculated when the diode current I_D becomes zero during switch-off mode prior to the next switch-on period. The boundary condition for DCM is $\xi \geq 1$ and calculated as:

$$\frac{RD}{fL_{eq}M^2} \geq 1 \quad (31)$$

The Eq. 31 can be used to find the minimum value of equivalent inductance L_{eq} required for the CCM operation of the MPOLC for given load resistance (R_L) and switching frequency (f) values (Pansare et al. 2017).

3. PROPOSED HYBRID INTELLIGENT CONTROLLER

Fuzzy logic control (FLC) is a popular method for performing MPPT in a PV system. Numerous studies (Tai et al. 2016) in the literature indicated that Type-1 FLC (T1FLC) did not display a high performance in highly uncertain situations in the system. On the other hand, a Type-2 FLC using Type-2 fuzzy sets displayed a better performance. In the present study, a hybrid intelligent controller, AIC IT2-TSKFLC, is proposed for the MPPT of a PV system with a combination of AIC algorithm and Type-2 FLC. The proposed hybrid intelligent controller is shown in Fig.4.

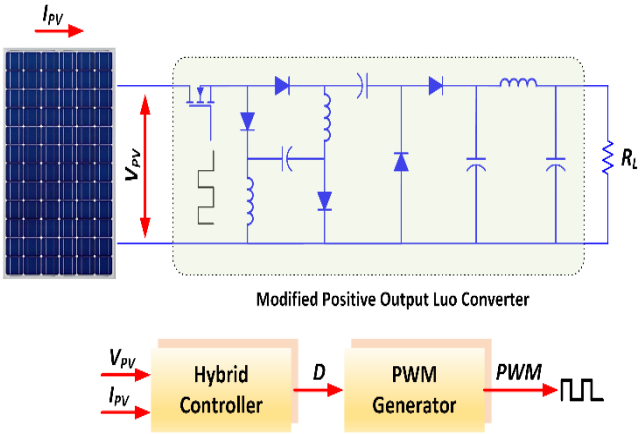

Figure 4. Proposed hybrid intelligent controller

As shown in Fig. 4, the proposed hybrid intelligent controller is used on the PV system consisting of a PV panel and MPOLC. Instantaneous voltage (V_{PV}) and current (I_{PV}) are calculated using PV panel using voltage and current sensors. The AIC algorithm is used to generate the error function of IT2-TSKFLC, which is responsible for the minimization of the error of MPP. IT2-TSKFLC calculates the duty ratio of the converter (D). The output of the proposed hybrid intelligent controller is applied to switching device of MPOLC via PWM generator. The control signal, which is the output of IT2-TSKFLC, is generated by Type-2 Fuzzy Sets. A Type-2 Fuzzy Set consists of triples $(x,u) : \mu_{\tilde{A}}(x,u)$ where x $\in$ X is a primary membership value, u $\in J_x$ (J_x represents the range of primary membership for a given x), and a secondary membership, $\mu_{\tilde{A}}(x,u)$ for each member of domain, can be expressed as follows:

$$\tilde{A} = \left\{ \left((x,u), \mu_{\tilde{A}}(x,u) \right) \mid \forall x \in X, \; \forall u \in J_x \subseteq [0,1], \mu_{\tilde{A}}(x,u) \in [0,1] \right\} \quad (32)$$

Footprint of uncertainty (FOU) in Fig. 5 is the limited domain corresponding to the primary uncertainty of Type-2 fuzzy set between upper ($\overline{\mu}_A$) and lower ($\underline{\mu}_A$) membership functions. It is assumed that FOU domain between upper and lower membership functions in Type-2 fuzzy set is an infinite Type-1 membership function. While the main properties of the general Type-2 fuzzy sets were preserved, interval Type-2 fuzzy sets were introduced as an alternative that reduces the computational burden (Mendel and John 2002). When all $\mu_{\tilde{A}}(x,u)$ is equal to 1, $\tilde{A}$ is an interval Type-2 fuzzy set. Interval Type-2 fuzzy sets can be defined as follows:

$$\tilde{A} = \left\{ \left((x,u), 1 \right) \mid \forall x \in X, \forall u \in J_x \subseteq [0,1] \right\} \quad (33)$$

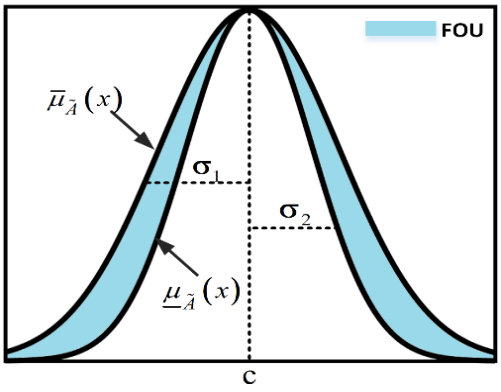

Figure 5. Gaussian type-2 fuzzy set

Both general and interval Type-2 fuzzy logic membership functions are three dimensional. However, they differ in terms of secondary membership function value of an interval Type-2 fuzzy logic function, which is equal to 1. Hence, their computational time is shorter compared to general Interval Type 2 Fuzzy Logic Controller (IT2-FLC). IT2-FLC consists of four parts: fuzzifier, rules & inference, type reducer and defuzzifier. The internal structure of IT2-FLC is shown in Fig. 6.

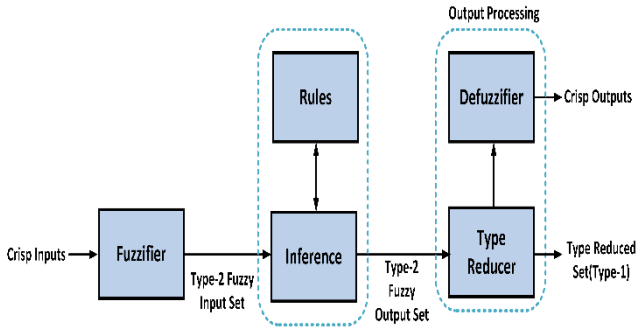

Figure 6. The internal structure of IT2-TSKFLC

In the present study, the antecedent parameters of IT2-TSKFLC are preferred as Type-2 fuzzy sets, and consequent parameters are selected as zero-order polynomials (Karnik et al. 1999). The rule base can be defined as:

$$R^k : IF\ \ x_1\ is\ \tilde{A}_1^{\,j}\ \ AND\ \ x_2\ is\ \tilde{A}_2^{\,n}$$
$$THEN\ \ R_k = p_k x_1 + q_k x_2 + r_k \qquad (34)$$

where k=1,2,….,25 denotes rule numbers, x_1, x_2 represent input variables (*e*, *de*), $\tilde{A}_1^{\,j}$ and $\tilde{A}_2^{\,n}$ are membership functions, R_k is the rule output and p_k , q_k , r_k are the consequent parameters. As shown in Fig. 5, Gaussian type membership function is used in the present study. The mathematical equations of Gaussian type membership function are given in Eqs. 35- 36.

$$\overline{\mu}_{A_i^j}(x_i) = \exp\left\{-\frac{1}{2}\left(\frac{x_i - c_{ij}}{\overline{\sigma}_{ij}}\right)^2\right\} \qquad (35)$$

$$\underline{\mu}_{A_i^j}(x_i) = \exp\left\{-\frac{1}{2}\left(\frac{x_i - c_{ij}}{\underline{\sigma}_{ij}}\right)^2\right\} \qquad (36)$$

Here, $\mu_{A_i^j}(x_i)$ is the degree of membership for input variable, c_{ij} denotes the mean value of function, σ_{ij} is standard deviation, and x_i is the input variable (Acikgoz et al. 2019). The controller proposed in the present study has two inputs (*e*, *de*) and a single output (*D*) which is duty ratio for DC-DC converter. The detailed structure of IT2-TSKFLC is shown in Fig. 7.

As shown in Fig. 7, IT2-TSKFLC configuration has seven layers.

Layer-1: This is the input layer. As shown in Fig. 4, the inputs of controller (*e*, *de*) are generated AIC algorithm using (V_{PV}, I_{PV}) values of PV panel and are described in Eq. 37. The characteristic curves of the AIC algorithm are shown in Fig. 8. It can be observed that the angle equals to zero around MPP point.

$$\tan^{-1}\left(\frac{I_{pv}}{V_{pv}}\right) + \tan^{-1}\left(\frac{dI_{pv}}{dV_{pv}}\right) = 0 \qquad (37)$$

Layer-2: This layer determines the degrees of the membership functions for inputs. The membership functions of the input and the rule base of the proposed hybrid intelligent controller must be determined based on MPP condition for IT2-TSK fuzzy inference system. The membership functions are labeled as (MF_1-MF_5), The membership functions are determined for error (*e*) and change of error (*de*) of the proposed hybrid control structure. Input membership functions are scaled based on a range of (-1, +1). Five Gaussian membership functions designed for the inputs are shown in Fig. 9.

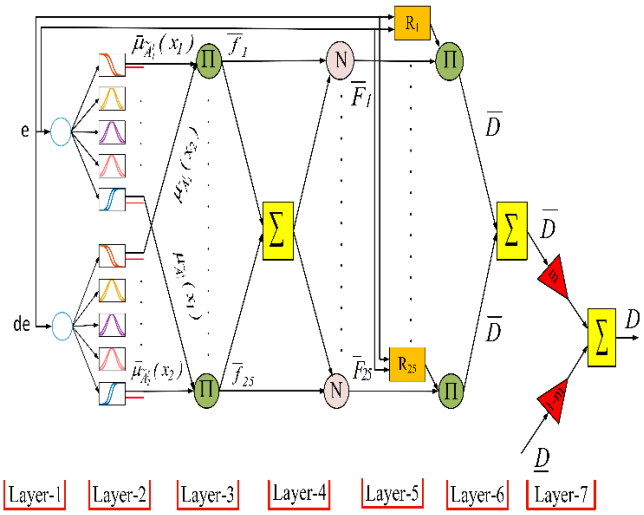

Figure 7. The structure of IT2-TSKFLC

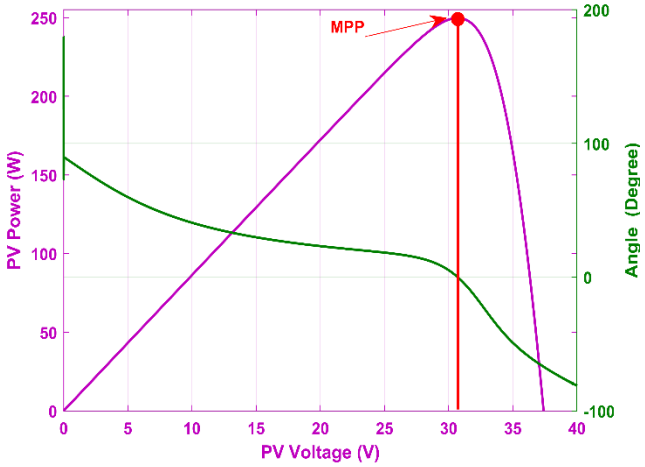

Figure 8. AIC angle curve and PV panel power compared with voltage characteristic curves

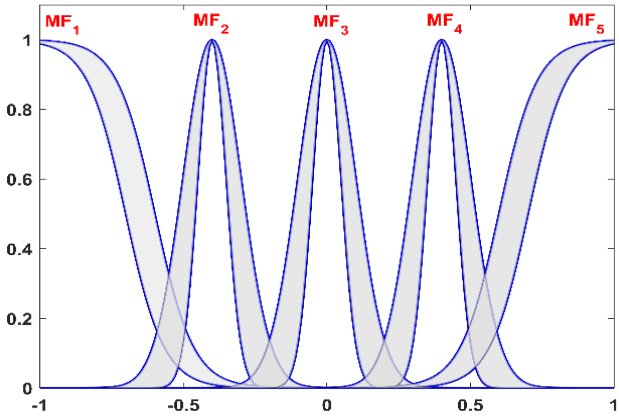

Figure 9. Five Gaussian membership functions designed for inputs

Layer-3: The third layer of the IT2-TSKFLC consists of the nodes represented by *Π*. The firing strengths of the

fuzzy rules are defined as lower and upper using product operator. The fuzzy rules of the proposed hybrid intelligent controller are presented in Table 1.The mathematical equations of the Layer-3 are calculated as:

$$\overline{f}_{(n-1)\times J+j} = \overline{\mu}_{A_1^j}(x_1) * \overline{\mu}_{A_2^n}(x_2) \quad n=1,2,\ldots,N \text{ and } k=(n-1)\times J+j \tag{38}$$

$$\underline{f}_{(n-1)\times J+j} = \underline{\mu}_{A_1^j}(x_1) * \underline{\mu}_{A_2^n}(x_2) \quad n=1,2,\ldots,N \text{ and } k=(n-1)\times J+j \tag{39}$$

Table 1. Fuzzy rules of proposed hybrid intelligent controller

D		de				
		MF$_1$	**MF$_2$**	**MF$_3$**	**MF$_4$**	**MF$_5$**
e	**MF$_1$**	R$_1$	R$_2$	R$_3$	R$_4$	R$_5$
	MF$_2$	R$_6$	R$_7$	R$_8$	R$_9$	R$_{10}$
	MF$_3$	R$_{11}$	R$_{12}$	R$_{13}$	R$_{14}$	R$_{15}$
	MF$_4$	R$_{16}$	R$_{17}$	R$_{18}$	R$_{19}$	R$_{20}$
	MF$_5$	R$_{21}$	R$_{22}$	R$_{23}$	R$_{24}$	R$_{25}$

MF: Membership Function R: Rule

Layer-4: This layer is also called the normalization layer, and each node is labeled as N. Normalization is calculated by proportioning the firing strength of each node rule to the sum of the firing strengths of all rules. This process can be expressed as:

$$\overline{F_k} = \frac{\overline{f_k}}{\sum \overline{f_k}} \qquad k=1,2,\ldots,25 \tag{40}$$

$$\underline{F_k} = \frac{\underline{f_k}}{\sum \underline{f_k}} \qquad k=1,2,\ldots,25 \tag{41}$$

Layer-5: It is a rule layer. The rule layer outputs are calculated based on the rule base. Layer outputs are calculated as:

$$R_k = p_k e + q_k de + r_k \quad k=1,2,\ldots,25 \tag{42}$$

Layer-6: The multiplication of membership degrees for upper and lower membership functions as well as linear functions is performed in this layer.

$$\overline{D} = \prod_{k=1}^{25} \overline{F_k}\,\overline{R_k} \tag{43}$$

$$\underline{D} = \prod_{k=1}^{25} \underline{F_k}\,\underline{R_k} \tag{44}$$

Layer-7: Biglarbegian-Melek-Mendel (BMM), which is a closed-form type reduction and defuzzification method, is used in this layer (Coteli et al. 2017). Closed mathematical form of type reduction and defuzzification process for the proposed IT2-TSKFLC is defined as:

$$D = m\frac{\sum_{k=1}^{25} \overline{f_k}\,\overline{R_k}}{\sum_{k=1}^{25} \overline{f_k}} + (1-m)\frac{\sum_{k=1}^{25} \underline{f_k}\,\underline{R_k}}{\sum_{k=1}^{25} \underline{f_k}} \tag{45}$$

4. SIMULATION STUDIES

The improved hybrid intelligent controller based on AIC-Interval Type-2 TSK Fuzzy Logic Controller for MPPT is simulated in MATLAB/Simulink environment using Sim Power System Toolbox. Solar irradiance and panel temperature values were obtained from a 10kWp real solar plant in Kahramanmaras. The performance and stability of the proposed control structure are analyzed under real environmental conditions.

4.1. Stand-Alone PV System and MPOLC Modelling

Single PV panel is used for simulation studies. The maximum power of a PV panel at the STC is 250W. Electrical characteristic parameters of the PV panel are given in Table 2. Calculated boundary circuit element values of the MPOLC using above mentioned design constraints are listed in Table 3. The MPOLC circuit element values in the simulation studies are selected higher than the calculated boundary circuit element values for a better continuous conduction mode (CCM) of operation.

Table 2. Electrical characteristic parameters of PV panel

Panel Type	Soltech STH-250-WH	
Optimum Operating Voltage	V_{MP}	30.7 V
Optimum Operating Current	I_{MP}	8.15 A
Open – Circuit Voltage	V_{oc}	37.4 V
Short – Circuit Current	I_{sc}	8.63 A
Maximum Power at STC	P_{max}	250 W
Panel Efficiency	η	15.4 %

Table 3. Calculated boundary circuit element values of MPOLC

V_s	30.7 V	L	0.23 mH
V_L	154.1 V	C_0	62.5 uF
R_L	100 Ω	C	15.61 uF
D	0.6	C_1	4.98 uF
L_o	0.015 mH	f	40 kHz
M	5.02	ζ_1	0.2
ζ	0.2	σ_1	0.01
σ	0.01	σ_2	0.01
σ_o	0.01	ζ_0	0.2
L_1	0.23 mH	C_2	62.74 uF

4.2. Simulation Results

The dynamic response of the proposed hybrid control structure is analyzed using real solar irradiance and panel temperature values. The actual values of solar parameters are obtained throughout a day from ta solar PV plant of power 10kWp installed in Kahramanmaras Sutcu Imam University. A view of solar PV plant is shown in Fig. 10. The actual solar irradiance and panel temperature values obtained from the solar PV plant on 22/08/2019 are shown in Figure 11.

Figure 10. A view of solar PV plant

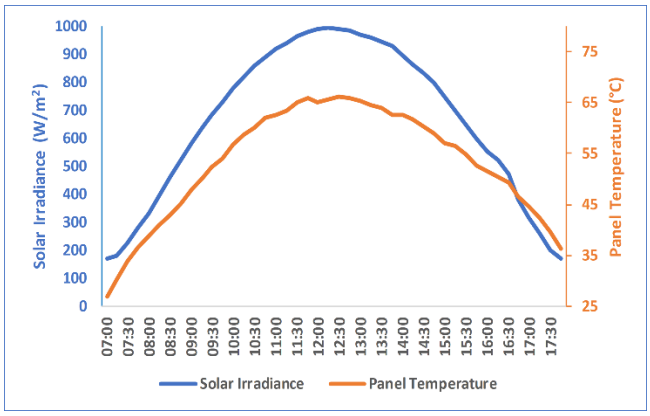

Figure 11. Daily variation of solar irradiance and panel temperature values

Actual values are sampled for the analysis of simulation studies. The sampled values are shown in Fig. 12(a). The output power curves of PV panel versus voltage are shown in Fig 12(b). It can be noted that sampled values and output power curves are analyzed under five different states for this simulation study.

Total simulation time was calculated as 0.3 s. State 1 indicates that solar irradiance and panel temperature values are fixed at 600 W/m^2 and 25˚C, respectively. The solar irradiance and panel temperature values were suddenly increased from 600 W/m^2 to 800 W/m^2 and 25˚C to 40˚C at t=0.1 s. Later, solar irradiance and panel temperature are increased in a similar manner to State 2. At the last two states, solar irradiance and panel temperature are decreased to represent the afternoon of a day for the analysis of MPP tracking performance of the proposed controller. As seen in Fig. 12(b), MPP power values of states are calculated 149.5 W, 187 W, 218 W, 172 W and 119 W, respectively.

Simulation results are given in Fig.13. It can be understood at the first state that PV power with conventional AIC method is 148.4 W, where PV power with the proposed control structure is 149.2 W.

The settling times of the proposed control structure and AIC method are 9.5 ms and 37.8 ms, respectively. At the second and third states of case, the MPP power of the PV panel was increased from 187 W to 218 W. PV power with AIC method was also increased from 186.1 W to 216.6 W. PV power with the proposed hybrid control structure was increased from 186.8 W to 217.9 W. At the last two states, MPP power of the PV panel was decreased from 172 W to 119 W. In addition, PV power with the proposed hybrid control structure was decreased from 171.8 W to 118.7 W, while PV power with AIC method was decreased from 170.8 W to 117.3W. As shown in Fig. 13(b), the proposed hybrid control structure successfully reduced the oscillation of the output power of DC-DC converter. PV power performance of both controllers were compared for all states in terms of transient performance indexes, and the results are summarized in Table 4.Maximum power efficiency demonstrates the extent to which the proposed controller can track MPP. The maximum power efficiency is calculated using ratio of the output power of the panel to the maximum power of the panel. The maximum power efficiencies of both controllers for all states are shown in Fig. 14.

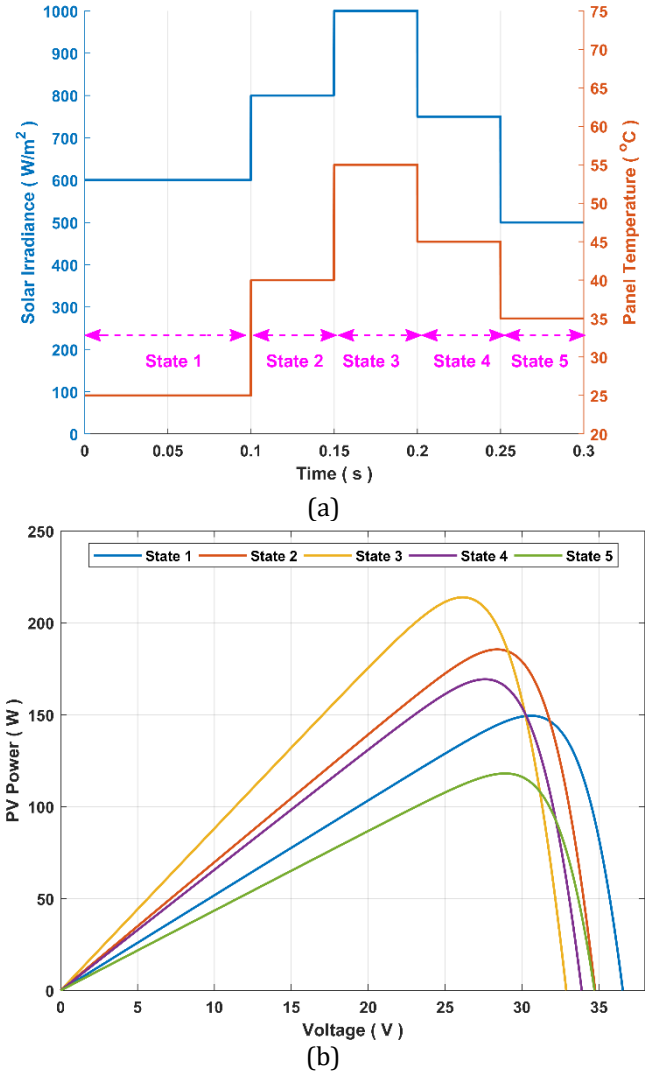

Figure 12. Solar irradiance and panel temperature (a) and PV power curves (b)

Table 4. Performance comparison of both controllers

All States	AIC - IT2-TSKFLC		AIC	
	Settling Time (ms)	Rise Time (ms)	Settling Time (ms)	Rise Time (ms)
State 1	9.5	1.37	37.8	1.53
State 2	3	0.11	28	17.5
State 3	2	0.12	16	9.5
State 4	2.7	0.09	30	4.8
State 5	5.2	0.09	49	4.2

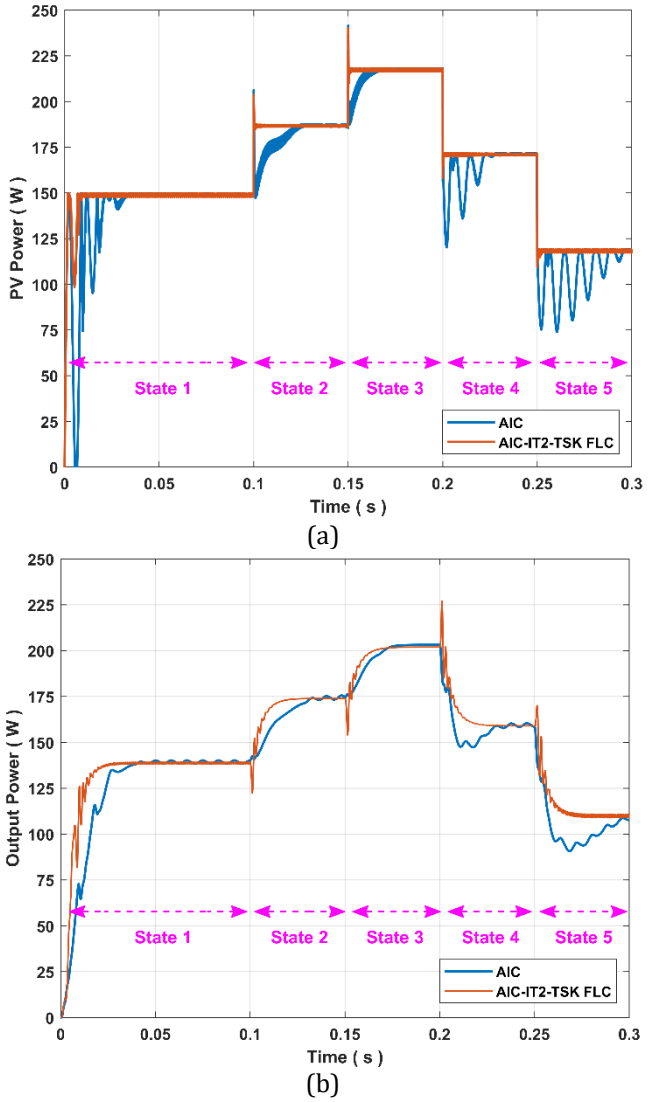

Figure 13. Output power responses of PV panel (a) and converter (b)

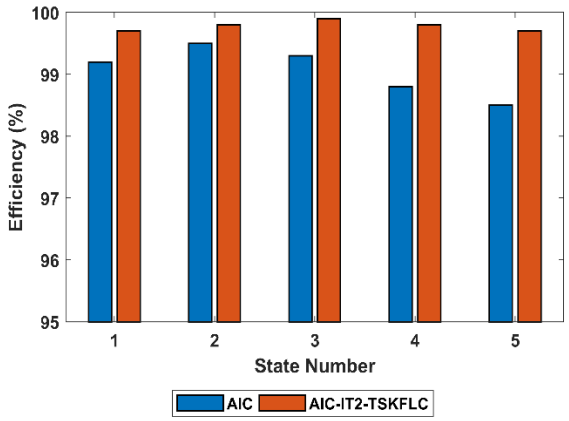

Figure 14. Maximum power efficiency comparison of both controllers

As seen in Fig. 14, the proposed hybrid control structure displays a higher performance compared to conventional AIC method in terms of maximum power efficiencies at all states. As a result, both controller methods extracted almost a maximum power from PV panel following the settling times for all states. While conventional AIC method has a long transient response for all states, the proposed control structure has a shorter transient response and a higher stability of PV power and converter output power. In addition, the proposed control structure tracked MPP values without any oscillation in PV power.

5. CONCLUSION

The present study proposed an improved hybrid control structure combined with AIC and IT2-TSKFLC for maximum power point tracking of a stand-alone PV system. MPOLC with a high voltage conversion gain was preferred for the PV system. IT2-TSKFLC consists of an effective and robust control structure that responded rapidly to unstable environmental conditions, and efficiently tracked MPP. Later, simulation studies were conducted for five different states to test the stability and dynamic performance of the proposed hybrid control structure. The hybrid control structure in the present study was compared with a conventional AIC method. The dynamic performance results obtained from five different states suggest that the proposed hybrid control structure ensured less oscillations and displayed a good steady state response on output powers of PV panel and MPOLC under unstable conditions. The proposed hybrid control structure has provided ms improvements. These improvements will contribute to the more stable and faster operation of the PV system. Furthermore, the proposed hybrid control structure improved its maximum power efficiency under rapidly changing environmental conditions.

ACKNOWLEDGEMENT

This work was financially supported by the Kahramanmaras Sutcu Imam University, Scientific Research Projects Unit, the project entitled “Optimal Control and Implementation of Maximum Power Point in Photovoltaic Systems” under Project No: 2018/5-11 D

REFERENCES

Acikgoz H, Kumar A, Beiranvand H & Sekkeli M (2019). Hardware implementation of type-2 neuro-fuzzy controller-based direct power control for three-phase active front-end rectifiers. International Transactions on Electrical Energy Systems, 29(10), 693-702. DOI: 10.1002/2050-7038.12066

Coteli R, Acikgoz H, Ucar F & Dandil B (2017). Design and implementation of Type-2 fuzzy neural system controller for PWM rectifiers. International Journal of Hydrogen Energy, 42(32), 20759-20771. DOI: 10.1016/j.ijhydene.2017.07.032

Dixit T V, Yadav A & Gupta S (2018). Experimental assessment of maximum power extraction from solar panel with different converter topologies. International Transactions on Electrical Energy Systems, 29(2), 1-33. DOI: 10.1002/etep.2712

Dogmus O, Kilic E, Sit S & Gunes M (2017). Adaptation of Optimized PID Controller with PSO Algorithm to Photovoltaic MPPT System. Kahramanmaraş Sütçü İmam University Journal of Engineering Sciences, 20(4), 1–8.

Karnik N N, Mendel J M & Liang Q (1999). Type-2 fuzzy logic systems. IEEE Transactions on Fuzzy Systems, 7(6), 643–658. DOI: 10.1109/91.811231

Kececioglu O F (2019). Robust control of high gain DC-DC converter using Type-2 fuzzy neural network controller for MPPT. *Journal of Intelligent & Fuzzy Syst*ems, 37(1), 941-651. DOI: 10.3233/JIFS-181770

Kececioglu O F, Acikgoz H & Gani A (2018). Fuzzy - PI Based MPPT Control for Photovoltaic Systems. Innovations in Intelligent Systems and Applications Conference (ASYU), Adana, Turkey. DOI: 10.1109/ASYU.2018.8554023

Kumbasar T (2016). Robust stability analysis and systematic design of single-input interval type-2 fuzzy logic controllers. IEEE Transactions on Fuzzy Systems, 24(3), 675–694. DOI: 10.1109/TFUZZ.2015.2471805

Luo F L (1997). Luo-converters, a series of new DC-DC step-up (boost) conversion circuits. Proceedings of Second International Conference on Power Electronics and Drive Systems, Singapore, 882-888. DOI: 10.1109/PEDS.1997.627511

Mendel J M & John R I B (2002).Type-2 fuzzy sets made simple. *IEEE Transactions on Fuzzy Systems*, 10(2), 117-127. DOI: 10.1109/91.995115

Ozdemir S, Altin N & Sefa I (2017). Fuzzy logic based MPPT controller for high conversion ratio quadratic boost converter. International Journal of Hydrogen Energy, 42(38), 17748-17759. DOI: 10.1016/j.ijhydene.2017.02.191

Pansare C, Sharma S K, Jain C & Saxena R (2017). Analysis of a modified positive output Luo converter and its application to solar PV system. IEEE Industry Applications Society Annual Meeting, Cincinnati, OH, USA, 1–6.

Radjai T, Gaubert J P, Rahmani L & Mekhilef S (2015). Experimental verification of P&O MPPT algorithm with direct control based on fuzzy logic control using CUK converter. International Transactions on Electrical Energy Systems, 25(12), 3492–3508. DOI: 10.1002/etep.2047

Soon T K & Mekhilef S (2015). A fast-converging MPPT technique for photovoltaic system under fast-varying solar irradiation and load resistance. IEEE Transactions on Industrial Informatics, 11(1), 176-186. DOI: 10.1109/TII.2014.2378231

Tai K, El-Sayed A R, Biglarbegian M, Gonzalez C I, Castillo O & Mahmud S (2016). Review of recent type-2 fuzzy controller applications. Algorithms, 9(2), 1-19. DOI: 10.3390/a9020039